Cytotoxic effects of the novel isoflavone, phenoxodiol, on prostate cancer cell lines

SIMON MAHONEY[1], FRANK ARFUSO[2], PIERRA ROGERS[2], SUSAN HISHEH[3], DAVID BROWN[4], MICHAEL MILLWARD[5] and ARUN DHARMARAJAN[2,*]

[1]*School of Biomedical Sciences, Faculty of Health Sciences, Curtin University, Kent Street, Bentley, Western Australia, Australia 6102*

[2]*School of Anatomy & Human Biology, The University of Western Australia, Perth, Western Australia, Australia 6009*

[3]*Department of Medicine – Austin Health and Northern Health, The University of Melbourne, Parkville, Victoria, Australia 3010*

[4]*Novogen Limited, 140 Wicks Road, North Ryde, NSW, Australia 2113*

[5]*School of Medicine and Pharmacology, The University of Western Australia, Perth, Western Australia, Australia 6009*

**Corresponding author (Fax, +61-8-64881051; Email, arunasalam.dharmarajan@uwa.edu.au)*

Phenoxodiol is an isoflavone derivative that has been shown to elicit cytotoxic effects against a broad range of human cancers. We examined the effect of phenoxodiol on cell death pathways on the prostate cell lines LNCaP, DU145 and PC3, representative of different stages of prostate cancer, and its effects on cell death pathways in these cell lines. Cell proliferation assays demonstrated a significant reduction in the rate of cell proliferation after 48 h exposure to phenoxodiol (10 and 30 μM). FACS analysis and 3′-end labelling indicated that all three prostate cancer cell lines underwent substantial levels of cell death 48 h after treatment. Mitochondrial membrane depolarization, indicative of early-stage cell death signalling, using JC-1 detection, was also apparent in all cell lines after exposure to phenoxodiol in the absence of caspase-3 activation. Caspase inhibition assays indicated that phenoxodiol operates through a caspase-independent cell death pathway. These data demonstrate that phenoxodiol elicits anti-cancer effects in prostate cancer cell lines representative of early and later stages of development through an as-yet-unknown cell death mechanism. These data warrant the further investigation of phenoxodiol as a potential treatment for prostate cancer.

[Mahoney S, Arfuso F, Rogers P, Hisheh S, Brown D, Millward M and Dharmarajan A 2012 Cytotoxic effects of the novel isoflavone, phenoxodiol, on prostate cancer cell lines. *J. Biosci.* **37** 73–84] **DOI** 10.1007/s12038-011-9170-6

1. Introduction

Adenocarcinoma of the prostate is the second most commonly diagnosed malignancy, and the most common cause of cancer-related death in men in Western countries (Hsing *et al.* 2000; Jemal *et al.* 2005). Prostate cancer characteristically progresses from a clinically localized androgen-sensitive primary tumour to androgen-independent metastatic disease. Prostate cancer cell proliferation is regulated by androgens via the androgen receptor (AR), which regulates the transcription of pro- and anti-apoptotic cell signalling. The androgen-independent phenotype of late-stage metastatic disease arises

Keywords. Apoptosis; isoflavone; phenoxodiol; prostate

Abbreviations used: AR, androgen receptor; FACS, fluorescence activated cell sorting; FCCP, carbonyl cyanide *p*-(trifluoromethoxy) phenylhydrazone; MTS, (3-(4,5-dimethylthiazol-2-yl)-5-(3-carboxymethoxyphenyl)-2-(4-sulpophenyl)-2H-tetrazolium); JC-1, 5,5′6,6′-tetrachloro-1,1′,3,3′-tetraethylbenzimidazolocarbocyanine iodide; RIPA, radioimmunoprecipitation assay; RT-PCR, reverse transcriptase polymerase chain reaction; SDS-PAGE, sodium dodecyl sulphate polyacrylamide gel electrophoresis

Published online: 8 January 2012

due to either increased AR expression and enhanced nuclear localisation of the AR, loss of AR function due to acquisitions of somatic mutations resulting in a more promiscuous receptor, or the up-regulation of anti-apoptotic proteins such as *Bcl-2* that circumvent the AR (Feldman and Feldman 2001). Treatment options such as chemotherapy for patients with late-stage metastatic prostate carcinoma rely on the premise that androgen-insensitive prostate carcinoma cells retain functional apoptotic machinery and have the potential to undergo programmed cell death. However, the inherent ability of tumour cells to avoid apoptosis is an underlying molecular reason contributing to disease progression and chemoresistance (Gleave *et al.* 2005).

Epidemiological studies have consistently shown an inverse association between isoflavone intake and the risk of cancer (Beecher 2003; Brown *et al.* 2005). *In vitro* mechanistic studies on isoflavones provide insight into potential modes of anti-cancer action ranging from cell cycle arrest and apoptosis induction to anti-angiogenic and anti-proliferative effects (Middleton *et al.* 2000; Brown *et al.* 2005).

Phenoxodiol, 2H-1-benzopyran-7-0,1,3-(4-hydroxyphenyl), is an isoflavone derivative that has been shown to elicit cytotoxic effects against a broad range of human cancers (Sapi *et al.* 2004; Aguero *et al.* 2005; Axanova *et al.* 2005; Brown *et al.* 2005; Silasi *et al.* 2009). Previous reports have indicated that phenoxodiol is a topoisomerase II inhibitor, inhibits sphingosine kinase activity, down-regulates transcription of angiogenic matrix metalloprotease 2 and other markers of angiogenesis, and can also induce apoptosis in chemoresistant ovarian cancer cells by regulating anti-apoptotic signalling pathways (Constantinou *et al.* 2003; Kamsteeg *et al.* 2003; Sapi *et al.* 2004; Aguero *et al.* 2005; Axanova *et al.* 2005; Brown *et al.* 2005; Gamble *et al.* 2005; Alvero *et al.* 2006). Phenoxodiol has been reported to inhibit cell proliferation in a wide range of human cancer cell lines and induce G1 cell cycle arrest as opposed to the G2-M arrest seen in similar flavanoid compounds like genistein (Alhasan *et al.* 1999; Aguero *et al.* 2005). It is postulated that phenoxodiol elicits its global anti-cancer activity by modulating the sphingomyelin pathway (De Luca *et al.* 2005; Morre *et al.* 2007). Recent data, however, have demonstrated that phenoxodiol is able to enhance perforin induced cell death elicited by T-cells in both *in vitro* and *in vivo* models of colon cancer (Georgaki *et al.* 2009).

Recent evidence has demonstrated that phenoxodiol augments the anti-cancer activity of cisplatin against the DU145 prostate cancer cell line both in *in vitro* and *in vivo* studies. An intracellular cisplatin accumulation assay showed a 35% ($p<0.05$) increase in the uptake of cisplatin when cells were treated with a combination of 1 μM cisplatin and 5 μM phenoxodiol, resulting in a 300% ($p<0.05$) increase in DNA adducts, hence explaining the sensitisation effect (McPherson *et al.* 2009). Here we investigated the phenoxodiol mechanism of action on LNCaP, DU145 and PC3 cells *in vitro* as monotherapy. We found phenoxodiol has direct cytotoxic effects over 48 h inducing early- and late-stage apoptosis. We also show that phenoxodiol induces apoptosis without the activation of caspase-3. These data suggest that phenoxodiol may have potential as a therapeutic agent in the treatment of prostate cancer.

2. Materials and methods

2.1 *Cell culture*

LNCaP (ATCC: CRL-1740), DU145 (ATCC: HTB-81) and PC3 (ATCC: CRL-1435) human prostate cells were all grown with 10% FBS, 2 mM L-glutamine and 1% penicillin/streptomycin media in a 5% CO_2 atmosphere at 37°C. LNCaP cells were grown in RPMI 1640 media (Gibco) supplemented with 10 mM HEPES, 2.5 g/L glucose and 1 mM sodium pyruvate. DU145 cells were grown in MEM with Earle's BSS media (Gibco) supplemented with 1 mM sodium pyruvate and 0.1 mM non-essential amino acids. PC3 cells were grown in Hams F12K media (Gibco).

2.2 *Phenoxodiol*

Phenoxodiol was made as a stock solution of 10 mg/mL in DMSO and stored at –20°C, protected from light. The stock was used within 7 days. The stock solution was diluted 100-fold in growth medium as a working dilution. This was then further diluted in growth medium to a final concentration of 10 μM or 30 μM. Vehicle control and 10 μM phenoxodiol treatment were augmented accordingly with DMSO to ensure uniform concentration.

2.3 *Cell proliferation assay*

Optimum seeding density for 96-well plates (Sarstedt) was determined and LNCaP cells were seeded at 30,000 cells/mL in 100 μL/well. DU145 cells were seeded at 15,000 cells/mL in 100 μL/well and PC3 cells were seeded at 25,000 cells/mL in 100 μL/well. Cells were grown for 48 h and then media aspirated and replaced with 100 μL of media containing the appropriate treatment. MTS proliferation analysis was performed 24 and 48 h post treatment using the Cell Titre 96 kit (Promega). Briefly, 20 μL of cell titre 96 were added to each well containing media and left for 3 h, and after 3 h, the absorbance was measured at 492 nm on a Labsystems Multiskan RC plate reader.

2.4 *DNA 3′-end labelling*

Seeding densities in 6-well plates were based on those determined for 96-well plates by adjusting for well surface area. Forty-eight hours post seeding, the medium was aspirated and replaced with medium containing vehicle control, 10 μM or 30 μM phenoxodiol. Cells were seeded at 54,000 cells/mL (LNCaP), 18,000 cells/mL (DU145) or 45,0000 cells/mL (PC3) in 2 mL of growth medium per well, in 6-well plates (Sarstedt). The methods of DNA extraction were undertaken as described previously (Dharmarajan *et al.* 1994). After extraction, purification and quantitation of the genomic DNA, the extent of apoptotic DNA internucleosomal fragmentation was determined by end-labelling using terminal transferase to bind radioactively labelled ddATP to 3′-ends of double- and single-stranded DNA. Methods used were those previously described (Korsmeyer *et al.* 2000). Briefly, 1 μg of DNA was incubated with reaction buffer, $CaCl_2$, terminal transferase (Roche) and [α-^{32}P] ddATP (Amersham). The reaction was terminated by EDTA followed by the addition of tRNA. DNA was then precipitated using ammonium acetate/ethanol and incubated at –80°C for 60 min. The DNA pellet was resuspended in 1x TE and DNA fragments separated on a 2% agarose gel. The extent of internucleosomal DNA fragmentation was observed by the incorporation of [α-^{32}P] ddATP onto the 3′-ends of low-molecular-weight (<20 kb) fragments. These low-molecular-weight bands were excised and quantified in a β-counter (Universal gamma counter, LKB WALLAC).

2.5 *FACS analysis*

Cells were seeded and treated as described for DNA 3′-end labelling. Following an appropriate incubation time (24 or 48 h), cells from each well were harvested by centrifuging the supernatant at 500*g* for 5 min and collecting floating cells. Adherent cells were trypsinized, transferred to a microcentrifuge tube and centrifuged at 500*g* for 5 min and then combined with corresponding floating cells. Cells were washed twice in 1x PBS and the supernatant removed. Cells were then incubated with Annexin-V-FLUOS (Roche)/Propidium Iodide (Sigma) solution in incubation buffer (10 mM HEPES/NaOH pH 7.4, 140 mM NaCl, 5 mM $CaCl_2$) for 10–15 min at room temperature in the dark. Additional control cells were also incubated as above with incubation buffer only, Annexin-V-FLUOS only or Propidium Iodide only to determine appropriate gate settings. Cells were diluted with 0.2 mL incubation buffer and sorted in a FACS Calibur Flow Cytometer (BD) to determine live, apoptotic and necrotic cell populations. To prevent clumping, cells were filtered through a 70 μM nylon mesh immediately prior to sorting.

2.6 *Caspase-3 activity assay*

Activation of effector caspases during apoptosis was determined using an Apo-One Homogenous Caspase-3/7 Assay Kit (Promega). Cells were seeded into black 96-well plates (Greiner Bio-One) at the appropriate density, as previously stated, in 100 μL media. Following 48 h incubation, phenoxodiol was added at concentrations from 0 μM (vehicle control), 10 μM and 30 μM and the cells incubated for a further 24 and 48 h respectively. The assay was terminated by the addition of 100 μL of reagent buffer and the luminescent signal measured after 1 h using a FLUOstar Optima plate reader set to 520 nm emission (BMG Laboratories, NSW, Australia). Appropriate blank and control samples were included in each run as recommended by the assay manufacturer.

2.7 *Caspase inhibition assay*

Inhibition of all caspase activity was determined using a general caspase inhibitor ZVAD-FMK (Chemicon) dissolved in DMSO. Cells were seeded in clear flat-bottomed 96-well plates (Greiner) at appropriate seeding densities, and grown for 48 h before the growth media was removed and replaced with growth media containing appropriate treatment. Following 48 h growth, cells were given either no treatment, vehicle control (DMSO), 10 μM ZVAD-FMK, 30 μM phenoxodiol or 10 μM ZVAD-FMK plus 30 μM phenoxodiol. DMSO levels were controlled for all groups except the negative control. After 48 h, 20 μL MTS dye (Promega) was added to each well and left for 3 h. After 3 h, the absorbance was measured at 492 nm on a Labsystems Multiskan RC plate reader.

2.8 *Detection of the mitochondrial potential sensor JC-1*

JC-1 is cationic dye that exhibits potential-dependent accumulation in mitochondria by fluorescence emission shift from green (~520 nm) to red (~590 nm). Consequently, mitochondrial depolarization is indicated by a decrease in the red–green fluorescence intensity ratio. Cells were seeded into white 96-well plates (Greiner Bio-One) at a density of 30,000 cells/mL in 100 μL media. Following 48 h incubation, phenoxodiol was added at concentrations from 0 (vehicle control), 10 μM and 30 μM and the cells were incubated for further 24 and 48 h respectively. The assay was terminated by aspirating the media and the addition of 50 μL of staining solution (33 μM JC-1 molecular probes in complete media without FBS) and the plates were incubated for 1 h at 37°C, 5% CO_2. In addition to the JC-1 stain, positive control cells were treated with 50 μM of carbonyl cyanide *p*-(trifluoromethoxy) phenylhydrazone (FCCP),

which results in depolarisation of the mitochondria. After FCCP addition, the red signal decreases rapidly as cells lose their potential, resulting in red–green ratio changes. The staining solution was then removed and 200 µL of PBS with 5% BSA were added. After a further 5 min incubation time, PBS/BSA was removed and 100 µL PBS were added. Analysis was performed on a FLUOstar optima plate reader (BMG Laboratories, NSW, Australia) with the filters set to 485 nm excitation/520 nm emission (green) and 544 nm excitation/590 nm emission (red). Data were presented as the ratio of red to green signals (590 nm/520 nm).

2.9 *Reverse transcription and quantitative RT-PCR*

Cells were seeded and treated as described for DNA 3′-end analysis. Cells floating in supernatant were centrifuged and combined with adherent cells per well. RNA was isolated using TriReagent (Astral Scientific) according to the manufacturer's instructions and then treated with DNA-*Free*™ (Ambion) according to the manufacturer's instructions, to remove contaminating genomic DNA. One microgram of RNA was reverse-transcribed using M-MLV (Promega) and random primers (Promega) according to the manufacturer's instructions. The resulting cDNA was purified (MoBio PCR clean-up kit) prior to real-time quantitative RT-PCR. Primers used to amplify *AIF, BAX, Bcl-xL, Caspase-3, xIAP* and *L19* (housekeeping gene) are outlined in table 1. RT-PCR was performed in 10 µL reactions using iQ SYBR green supermix (Biorad) and 1 µL cDNA in the Rotor-Gene 3000 (Corbett Research). Cycling conditions were 95°C (0–45 s), annealing temperature as per table 1 (15–45 s) and 72°C (5–45 s) for 45 cycles. Amplification was confirmed by melt curve analysis and by electrophoresis in 2% agarose/ethidium bromide for product size. Threshold cycle values for cDNA samples were compared against a standard curve obtained by amplification of tenfold dilutions of corresponding PCR product. Each cDNA sample was run in duplicate and an average obtained. All mRNA levels were normalized by dividing by L19 mRNA levels for each cDNA sample.

2.10 *Western blot analysis*

Cells were homogenized in RIPA buffer (150 mM NaCl, 50 mM Tris-HCl pH 7.5, 1% Triton X-100, 0.5% sodium deoxycholate, 0.1% SDS, 0.1 mM PMSF). Protein concentration of homogenates was measured using the Bradford assay and 30 µg resolved by 12% SDS-PAGE and transferred to nitrocellulose membranes (Amersham). Membranes were blocked in 5% non-fat milk in Tris buffer solution with 0.5% Tween 20 (TBS-T) for 30 min at 37°C. Membranes were then incubated in primary antibody overnight at 4°C as follows: 1:1000 in TBS-T (AIF: Cayman, #160773), 1:200 in TBS-T (Bax: Abcam, #7977), 1:200 (Bcl-xL: Abcam, #7974) and 1:250 in 3% non-fat milk in TBS-T (XIAP: Transduction Laboratories, #610762). With the exception of Bcl-xL, membranes were incubated in the appropriate secondary antibody (1:10,000 HRP-linked) for 1 h at room temperature. Bcl-xL membranes were incubated in 1:10,000 biotinylated secondary antibody for 1 h at room temperature followed by 30 min in streptavidin-HRP complex. Membranes were incubated in ECL substrate (Pierce) before exposure to ECL Hyperfilm (Amersham). To normalize signals to β-actin, membranes were stripped, washed in TBS-T and then blocked in 5% non-fat milk in TBS-T for 30 min at 37°C. This was followed by incubation in β-actin antibody (1:5000 in TBS-T: Sigma) overnight at 4°C, followed by 1 h incubation in appropriate secondary antibody (1:10,000 HRP-linked) at room temperature. Membranes were then incubated in ECL substrate before exposure to ECL Hyperfilm. Signals were quantified by densitometry using Scion Image and measures of *AIF, Bax, Bcl-xL* and *XIAP* were standardized to measures of β-actin for each sample.

2.11 *Data presentation and statistics*

Data are presented as mean±SEM. For each experiment *n* is indicated in figure legends and refers to the number of well replicates per group. Differences between control and

Table 1. Primers used in the present study, their sequence, expected amplicon size and annealing temperature

	Primer forward	Primer reverse	Product size	Annealing temperature (°C)
AIF	5′-GAT CAC GCT GTT GTG AGT GG-3′	5′-TCT TGT GCA GTT GCT TTT GC-3′	179 bp	61
BAX	5′-GCT GGA CAT TGG ACT TCC TC-3′	5′-TCA GCC CAT CTT CTT CCA GA-3′	167 bp	61
Bcl-xL	5′-ACA ATG CAG CAG CCG AGA G-3′	5′-ATG TGG TGG AGC AGA GAA GG-3′	167 bp	61
Caspase-3	5'-AAA GGA TCC TTA ATA AAG GTA TCC ATG GAG AAC ACT-3'	5'-AAA GAA TTC CAT CAC GCA TCA ATT CCA CAA TTT CTT-3'	322 bp	55
XIAP	5'-GGG GTT CAG TTT CAA GGA CA-3'	5'-CGC CTT AGC TGC TCT TCA GT-3'	183 bp	56
L19	5'-CTG AAG GTC AAA GGG AAT GTG-3'	5'-GGA CAG AGT CTT GAT GAT CTC-3'	194 bp	52

treatment group means were measured by two-sample *t*-tests. Statistical significance is $p<0.05$.

3. Results

3.1 *MTS assay*

Proliferation assays (MTS) of the LNCaP, DU145 and PC3 cell lines indicated significant decreases in proliferation, particularly at 48 h exposure (figure 1).

3.2 *DNA 3′-end labelling*

Following end-labelling and electrophoresis, the presence of a DNA ladder was observed in LNCaP and DU145 cells following phenoxodiol treatment at both 24 and 48 h (figure 2). The DNA was quantified to determine the extent of apoptotic labelling. LNCaP cells had a significant increase in apoptotic DNA fragmentation after 24 h treatment with 10 μM ($p=0.006$) and 30 μM phenoxodiol ($p=0.05$), while over 48 h only 30 μM treatment produced a significant increase in apoptosis ($p=0.044$) (figure 2A). DU145 cells had a significant increase in DNA labelling after 24 h with a 30 μM treatment ($p=0.024$), while over 48 h both 10 μM and 30 μM phenoxodiol concentrations induced significant increases in apoptotic DNA fragmentation ($p<0.001$, $p=0.033$) (figure 2B). PC3 3′-end labelling indicated a necrotic response in the samples, and therefore, DNA end-labelling was not quantified

3.3 *FACS analysis*

The use of the double stain of Annexin-V-FLOUS and Propidium Iodide allows separation between live cell populations, cells entering early apoptosis and those in late-stage apoptosis/necrosis. Any late-stage apoptosis has been labelled as necrosis because this technique is not sensitive enough to differentiate between the two. In LNCaP cells, 24 h exposure to phenoxodiol did not produce significant cell death (figure 3A). After 48 h, however, a significant reduction in live cells was observed using 10 μM phenoxodiol ($p=0.001$). Cells appeared to be dying by both an apoptotic and necrotic response as both populations increased significantly after 48 h of 10 μM ($p=0.01$ apoptotic, $p=0.001$ necrotic) and 30 μM ($p=0.13$ apoptotic, $p=0.03$ necrotic) phenoxodiol treatment (figure 3A). The extent of apoptosis is different between 3′-end DNA Fragmentation versus FACS analysis. Both are qualitative and quantitative measures; however, DNA fragmentation assays take into account all the apoptosis that has occurred up until that point in time (in this case 24 h of total apoptosis), while FACS takes into account only the ratio of early to late apoptosis that has occurred at the point of preparation for the technique. Included in that is also the ability of FACS analysis to screen and select populations of

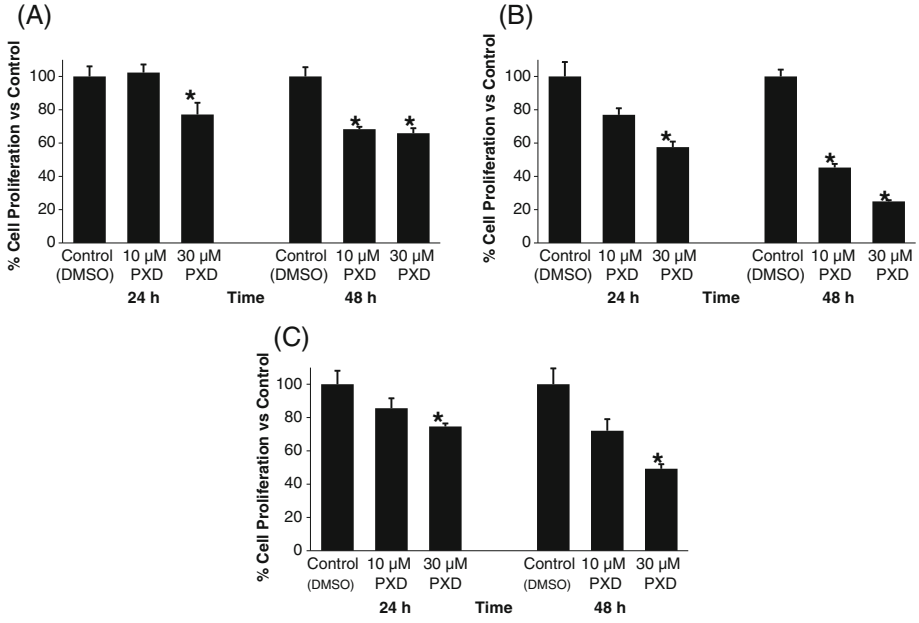

Figure 1. MTS Analysis of LNCaP (**A**), DU145 (**B**) and PC3 (**C**) cell lines. Data expressed as mean±SEM, $n=4$ per time/dose point. Data represented are cell data minus mean of no cell controls ($n=3$) as phenoxodiol reacts with MTS increasing absorbance. * $p<0.05$ relative to control.

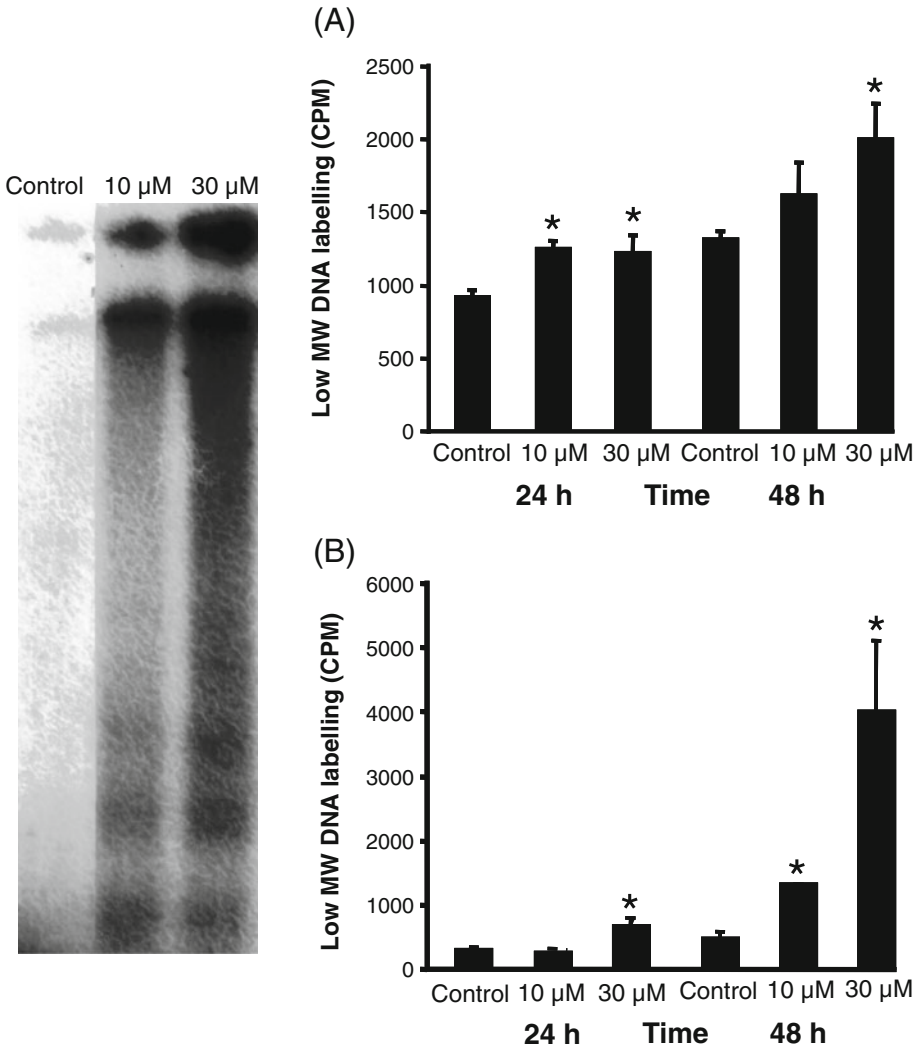

Figure 2. 3′-End labelling apoptosis analysis of LNCaP (**A**) and DU145 (**B**) phenoxodiol treated cells over 24 and 48 h. Genomic DNA extracted from LNCaP cultured cells analysed by autoradiography after 48 h (left panel); and beta-counting of low molecular weight (<15 kb) DNA fragments (right panel). PC3 cells were found to be necrotic in response to phenoxodiol and were not quantitated using this method. Data expressed as mean ± SEM, $n=3$ per time/dose point. *$p<0.05$ relative to control for the occurrence of internucleosomal cleavage associated with apoptosis.

single cells in media, whereas fragmentation analysis utilizes all cells.

DU145 cells exhibited a minor increase in apoptosis over 24 h in response to both 10 μM ($p=0.044$ apoptotic, $p<0.001$ necrotic) and 30 μM ($p<0.001$ apoptotic) phenoxodiol concentrations. After 48 h exposure, DU145 cells exhibited a significant, linear increase in both apoptotic and necrotic cell death between 10 μM ($p<0.001$ apoptotic, $p=0.002$ necrotic) and 30 μM ($p<0.001$ apoptotic, $p\leq0.001$ necrotic) phenoxodiol treatments with a corresponding significant linear decrease in viable cells when compared to control (figure 3B).

The response of PC3 cells to phenoxodiol was different from that of LNCaP and DU145 with no increase in apoptotic cell death and a linear increase in late-stage apoptosis/necrosis, which is consistent with the lack of apoptotic laddering in the DNA 3′-end labelling of this cell line. Over 24 h cell death was increased in a dose-dependent manner with a resulting decrease in live cell population with both 10 μM ($p<0.001$ live cells, $p<0.001$ necrotic) and 30 μM phenoxodiol treatment ($p<0.001$ live cells, $p<0.001$ necrotic) (figure 3C). After 48 h, treatment groups had profiles similar to that found in the 24 h treatment group, with cell death exhibiting a dose-dependent response and a resultant decrease in live cell population: 10 μM ($p<0.001$ live cells, $p<0.001$ necrotic) and 30 μM ($p<0.001$ live cells, $p<0.001$ necrotic). The decrease in the small

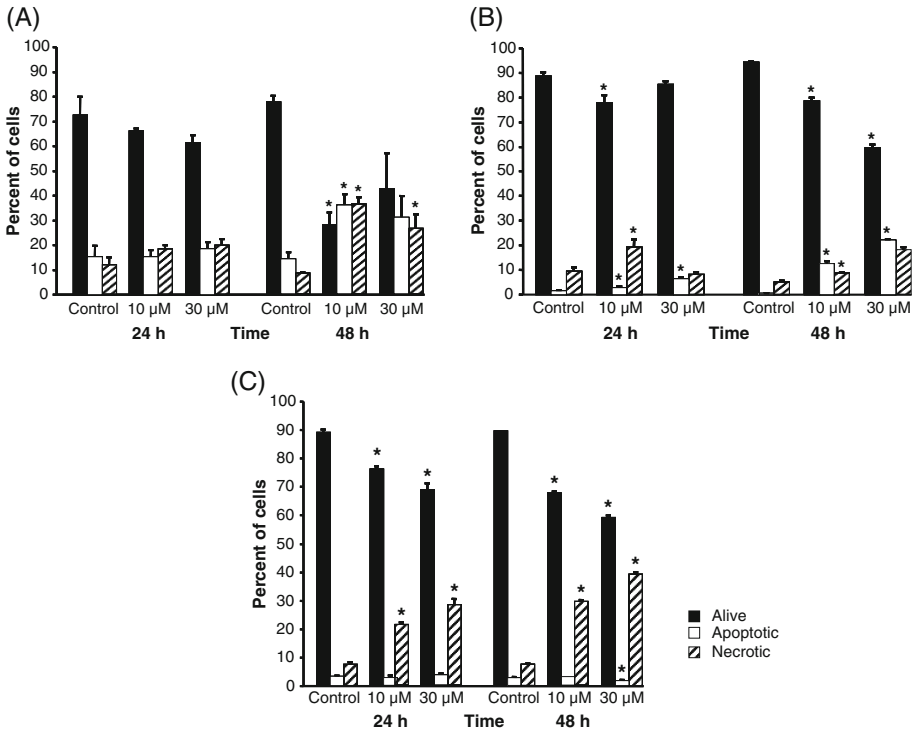

Figure 3. FACS analysis of phenoxodiol induced apoptosis using Annexin V and Propidium Iodide double staining. LNCaP (**A**), DU145 (**B**) and PC3 (**C**) cells were treated over 24 and 48 h. Data expressed as mean ± SEM, $n=3$ per time/dose point. *$p<0.05$ relative to control.

apoptotic population, seen after 48 h with the 30 μM phenoxodiol treatment group ($p=0.019$), is related to the 30% decrease in live cell population as compared to the control (figure 3C).

3.4 *Caspase-3 activity assay*

The caspase-3 activity assay for LNCaP cells indicated no significant changes in caspase-3 expression over 24 h. However, a significant reduction in caspase-3 expression was noted after 48 h at both 10 μM ($p=0.004$) and 30 μM phenoxodiol treatment ($p=0.001$) (figure 4A). DU145 cells exhibited no significant changes in caspase-3 expression over 24 h but a significant, if slight, increase over 48 h with both 10 μM ($p=0.009$) and 30 μM phenoxodiol doses ($p=0.016$) (figure 4B). PC3 cells did not indicate any change in activated caspase-3 expression over any time point (data not shown). These data clearly implicate a lack of consistent signalling between the three cell lines and correlate with the FACS and 3′-end DNA labelling data, suggesting that phenoxodiol induces apoptosis in some cells and necrosis in others, although it is important to note the changes are far smaller than expected for a drug that invokes caspase-mediated apoptosis.

3.5 *Caspase inhibition assay*

Cell proliferation assays demonstrated that co-culturing all three prostate cancer cells with a pan caspase inhibitor (ZVAD-FMK, 10 μM) and phenoxodiol (30 μM) failed to prevent the anti-proliferative activity of phenoxodiol (figure 5A, B and C), with all three cell lines exhibiting significant reduction in cell proliferation ($p<0.05$) over a 48 h period. This indicates that phenoxodiol is able to induce caspase-independent cytotoxicity in prostate cancer cells where the classical apoptosis pathway has been inhibited.

3.6 *JC-1 Assay*

All three cell lines demonstrated statistically significant mitochondrial depolarization, indicative of early stage cell death signalling, over both 24 and 48 h time points (figure 6). Importantly, the extent of depolarization varies between the cell lines with LNCaP and DU145 having a far greater rate of depolarization compared to PC3. These results confirm the proliferation and apoptosis assays by demonstrating large depolarization in the two cell lines that responded apoptotically to phenoxodiol treatment, LNCaP and DU145. PC3 cells were only slightly depolarized as

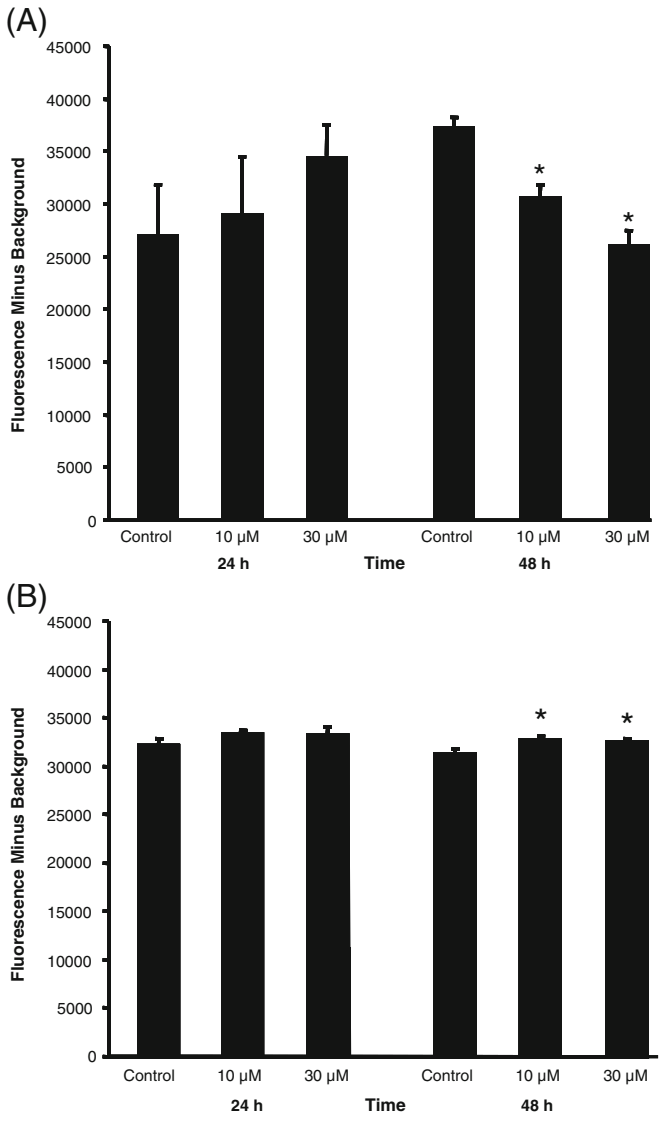

Figure 4. Caspase-3 activity assay of LNCaP (**A**) and DU145 (**B**) cells treated with phenoxodiol over 24 and 48 h. PC3 cells had no significant change in Caspase-3 levels. Data expressed as mean minus background at 520 nm ± SEM, $n=4$ per time/dose point. *$p<0.05$ relative to control.

expected because of the lack of apoptosis in response to treatment. In LNCaP and DU145 cells, treatment over 24 h with 30 μM phenoxodiol resulted in a significantly reduced ratio ($p=0.01$ and $p<0.001$), while in the 48 h treatment the ratio was significantly decreased at both 10 μM ($p=0.02$ and $p=0.001$) and 30 μM phenoxodiol treatments ($p<0.001$ and $p<0.001$) (figure 6A and B). PC3 cells exhibited significant depolarization in both treatments across 24 h ($p=0.03$ and $p=0.012$) and 48 h ($p=0.018$ and $p=0.002$) (figure 6C). However, the total overall ratio reduction for treatment versus control was not as great as that exhibited by LNCaP and DU145 cells.

3.7 *Quantitative RT-PCR*

Quantification of apoptosis-related gene transcripts (*AIF*, *BAX*, *Bcl-xL*, *Caspase-3* and *XIAP*) in phenoxodiol-treated prostate cells was analysed. No significant differences in the mRNA levels between control and treatment were detected for *Bax*, *Bcl-xL* and *XIAP* in all three cell lines (data not shown).

3.8 *Western blot analysis*

Western blot analysis of the AIF, Bax, Bcl-xL and XIAP whole-cell protein expression indicated no consistent significant changes in protein expression between the three cell lines (data not shown).

4. Discussion

We show here using the MTS viability assay that phenoxodiol elicits time- and dose-dependent anti-proliferative activity against both androgen-responsive and androgen-resistant prostate cancer cell lines.

Classic apoptosis, such as that induced by chemotherapeutic agents, can proceed via extrinsic death-receptor-mediated and intrinsic mitochondrial-mediated pathways ultimately resulting in the activation of caspase-3. Members of the BH3 family such as Bcl-2 and Bcl-xL are anti-apoptotic and maintain mitochondrial membrane integrity by binding mitochondrial porin channels. These anti-apoptotic proteins also protect cells from apoptosis by binding to pro-apoptotic BH3 only members, such as Bid and Bax (Korsmeyer *et al.* 2000; Cheng *et al.* 2001; Cory and Adams 2002; Puthalakath and Strasser 2002). Alternatively, members of the Inhibitors of Apoptosis Proteins (IAP) such as XIAP prevent apoptosis by inactivating caspase-3 and caspase-9. FLICE inhibitory protein (FLIP) binding to caspase-8 can also prevent death receptor-mediated apoptosis.

To elucidate the mechanism by which phenoxodiol elicits an anti-proliferative effect in prostate cancer cell lines, we investigated the kinetics of apoptosis induction. Through use of 3′-end labelling and Annexin-V-PI-based FACS analysis, we demonstrated that phenoxodiol induced cell death in 2 of 3 cell lines via classic apoptosis-induced DNA fragmentation and externalization of phosphatidyl serine. In contrast, phenoxodiol retarded the proliferation of PC3 cells in the absence of DNA laddering and externalization of phosphatidylserine. FACS analysis showed that phenoxodiol clearly induced the appearance of apoptotic and late-

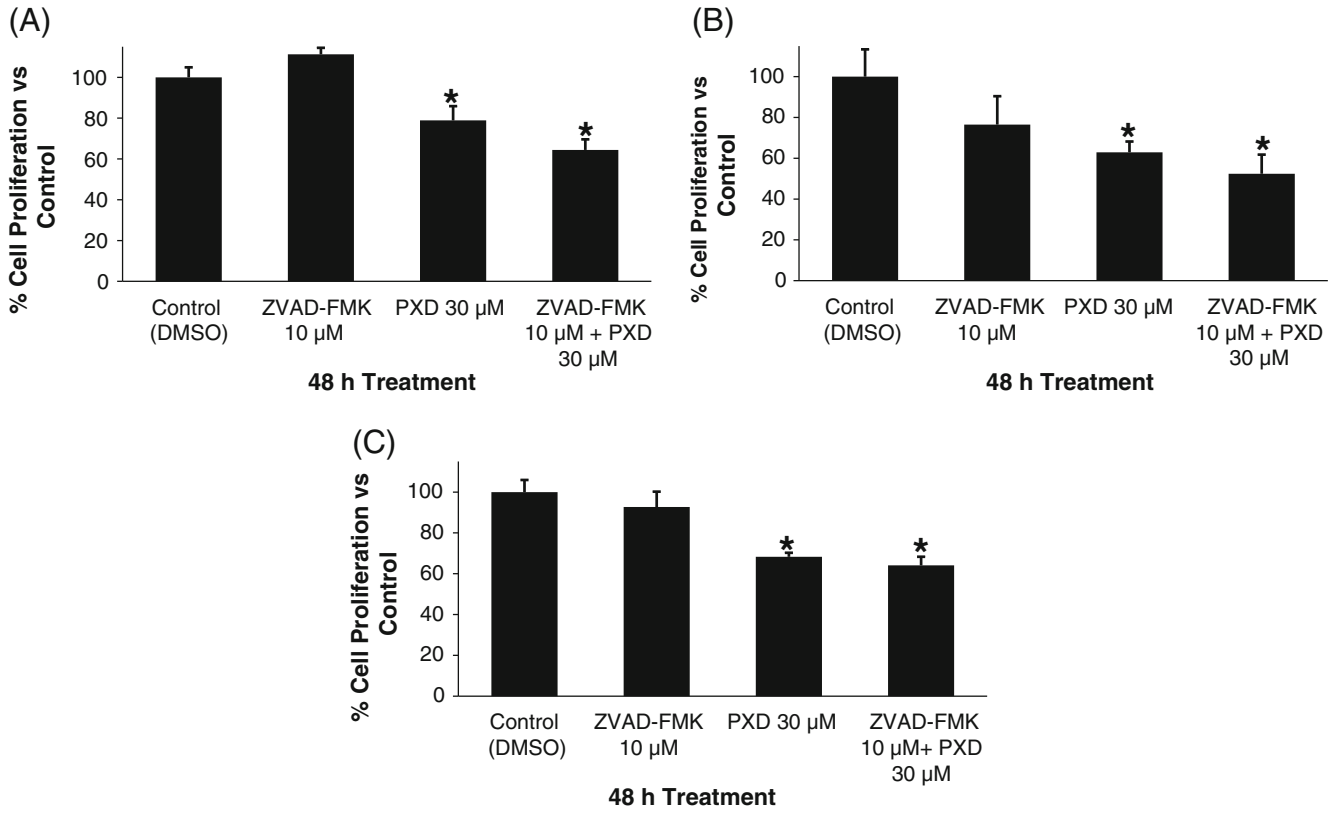

Figure 5. Caspase inhibition assay of LNCaP (**A**), DU145 (**B**) and PC3 (**C**) cells treated with 30 μM phenoxodiol and 10 μM ZVAD-FMK over 48 h. MTS treatment following time point reached. Data expressed as mean minus no cell control background at 492 nm absorbance ± SEM, $n=4$ per time/dose point. *$p<0.05$ relative to control.

stage apoptotic/necrotic populations of cells, as well as a marked decrease in viable cells. All three cell lines responded to phenoxodiol treatment with a minimum of a 30% decrease in viable cells after 48 h and a variable incidence of early apoptotic and late-stage apoptotic/necrotic cell populations. In all modes of analysis, cell death was reliant on dose and duration of phenoxodiol exposure. Investigation of phenoxodiol induced changes to mitochondrial membrane potential by the use of the JC-1 assay suggested that phenoxodiol elicited apoptosis via mitochondrial catastrophe in LNCaP and DU145 cells, which was dose- and duration-dependent. Unlike LNCaP and DU145, PC3 cells displayed a necrotic response to phenoxodiol and a large increase in mitochondrial depolarization was not observed. Furthermore, caspase-3 was not activated in phenoxodiol treated PC3 cells, nor were any consistent changes in the expression of key apoptosis proteins observed, indicating that PC3 cells were undergoing cell death via an alternate route. These data demonstrate that phenoxodiol causes a dose response in terms of reduced cell viability in androgen-insensitive DU145 and PC3 cell lines and in androgen-sensitive LNCaP cells over 48 h. Given that phenoxodiol induced classic apoptosis in ovarian cancer (Gamble *et al.* 2005; Alvero *et al.* 2006), it was surprising to find that caspase-3 expression remained unchanged in PC3 cells and even declined in LNCaP cells, while the actual increase in expression in DU145 cells was minimal. The lack of caspase-3 activation within the first 24 h of phenoxodiol treatment and the inability of a pan-caspase inhibitor to prevent the anti-proliferative activity of phenoxodiol in all three cell lines suggests that the phenoxodiol mechanism of cell death in prostate cancer occurs via a caspase-independent pathway.

The cytotoxicity of phenoxodiol was not associated with changes in both pro-apoptotic and anti-apoptotic members of the Bcl-2 family. The ratio of pro-apoptotic Bax protein to anti-apoptotic protein Bcl-xL can be a determinant of cellular susceptibility to apoptosis. Prostate cancer has been shown to express Bcl-2 family members (Scherr *et al.* 1999) as well as having changes in the ratio of signalling with treatment (Tang *et al.* 2006). However, a lack of change has also been previously reported in clonogenic studies (Tannock and Lee 2001). Modulation of other pro- or anti-apoptotic proteins also remained un-

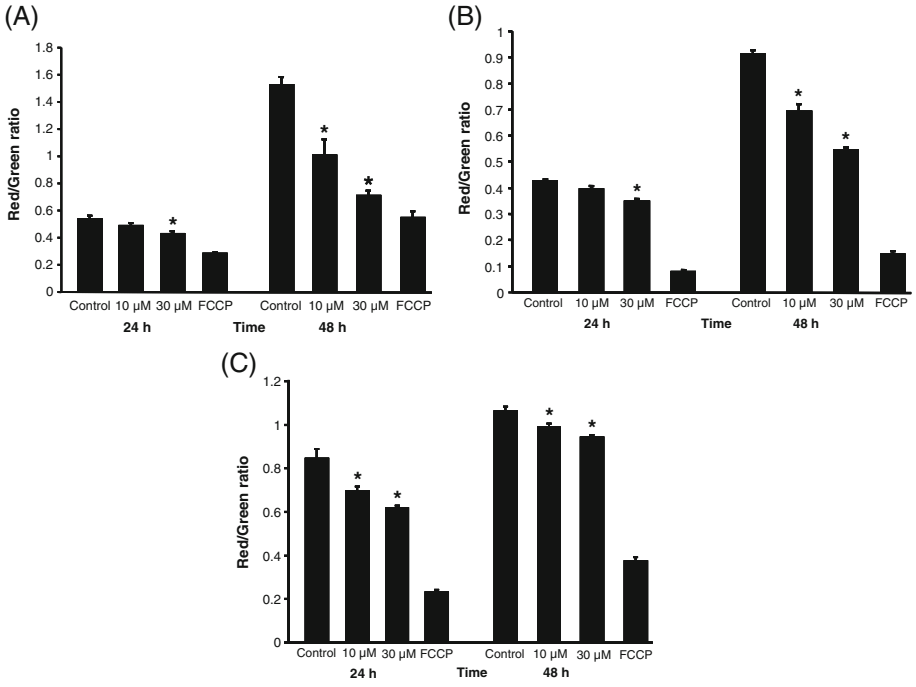

Figure 6. JC-1 Mitochondrial potential assay of LNCaP (**A**), DU145 (**B**) and PC3 (**C**) cells treated with phenoxodiol over 24 and 48 h. Data expressed as mean of 590 nm/520 nm emission spectrum ± SEM, $n=4$ per time/dose point. *$p<0.05$ relative to control.

changed, indicating that phenoxodiol could be inducing cell cycle arrest through mitotic catastrophe or premature senescence, which arrests cell replication permanently. Phenoxodiol-mediated cell death was not linked to a caspase-independent pathway, which would have been indicated via AIF signalling. AIF induces caspase-independent cell death primarily through translocation from the mitochondria to the nucleus where it mediates chromatin condensation and high-molecular-weight fragmentation of DNA (Hong *et al.* 2004). The lack of a consistent change in gene expression between LNCaP, DU145 and PC3 cell lines indicates that phenoxodiol does not promote cell death by disrupting the stoichiometry of key pro- and anti-apoptotic molecules in prostate cancer cells.

The common model for cancer therapy activity has been that anti-cancer regimens cause apoptotic signalling to occur, often mediated by p53 and caspase-3 up-regulation (Fojo and Bates 2003). Therefore, cells that are resistant to apoptosis achieve this through forced overexpression of anti-apoptosis molecules such as XIAP and Bcl-xL family members or p53 mutation (Brown and Attardi 2005). These data are in contrast to those in other reports where it has been demonstrated in ovarian cancer that caspase activation, Bax up-regulation and XIAP degradation are key proteins modulated by phenoxodiol (Sapi *et al.* 2004; Alvero *et al.* 2006). Recent reports indicate that, in addition to apoptosis, cells can be effectively eliminated through necrosis, mitotic catastrophe and premature senescence, which results in cell cycle arrest and subsequent cell death signalling (Brown and Wouters 1999; Brown and Wilson 2003; Tannock *et al.* 2004).

Cells that are non-responsive to treatment through the classic intrinsic apoptosis pathways, yet have an apoptotic response, must activate this process through other mechanisms such as mitochondrial response and depolarization, mitotic catastrophe and DNA degradation (Ruth and Roninson 2000; Brown and Wilson 2003). Additionally, cells can undergo apoptosis through mechanisms such as cytochrome-c release, caspase-8 and caspase-9 signalling as well as high-molecular-weight DNA breakdown. Indeed, it would appear from our studies in cell lines representative of different phases of prostate cancer that phenoxodiol elicits an alternative, and as yet unidentified, mode of cell death. These data indicate that phenoxodiol can elicit significant anti-cancer and cytotoxic effects upon prostate cancer in varying stages including the early clinical stage of development.

Phenoxodiol exhibits significant ability to induce cell death in the prostate cancer cell lines LNCaP, DU145 and PC3 that utilize different signalling pathways than those reported in ovarian cancer studies and clearly demonstrates cell-death-inducing capabilities on cancer cells. Coupled with the induction of apoptotic cell death through non-classical pathways, phenoxodiol shows potential as a drug for future treatment of prostate cancer.

Acknowledgements

The authors would like to acknowledge the technical help of Mr Greg Cozens from the School of Anatomy and Human Biology, University of Western Australia, and Dr Kathy Heel from the Centre for Microscopy, Characterisation and Analysis. The authors acknowledge the facilities, scientific and technical assistance of the Australian Microscopy & Microanalysis Research Facility at the Centre for Microscopy, Characterisation & Analysis, The University of Western Australia, a facility funded by The University, State and Commonwealth Governments. AD is supported by the Cancer Council of Western Australia. This study was supported by Novogen Ltd.

References

Aguero MF, Facchinetti MM, Sheleg Z and Senderowicz AM 2005 Phenoxodiol, a novel isoflavone, induces G1 arrest by specific loss in cyclin-dependent kinase 2 activity by p53-independent induction of p21WAF1/CIP1. *Cancer Res*. **65** 3364–3373

Alhasan SA, Pietrasczkiwicz H, Alonso MD, Ensley J and Sarkar FH 1999 Genistein-induced cell cycle arrest and apoptosis in a head and neck squamous cell carcinoma cell line. *Nutr. Cancer* **34** 12–19

Alvero AB, O'Malley D, Brown D, Kelly G, Garg M, Chen W, Rutherford T and Mor G 2006 Molecular mechanism of phenoxodiol-induced apoptosis in ovarian carcinoma cells. *Cancer* **106** 599–608

Axanova L, Morre DJ and Morre DM 2005 Growth of LNCaP cells in monoculture and coculture with osteoblasts and response to tNOX inhibitors. *Cancer Lett*. **225** 35–40

Beecher GR 2003 Overview of dietary flavonoids: nomenclature, occurrence and intake. *J. Nutr*. **133** 3248S–3254S

Brown JM and Attardi LD 2005 The role of apoptosis in cancer development and treatment response. *Nat. Rev. Cancer* **5** 231–237

Brown JM and Wilson G 2003 Apoptosis genes and resistance to cancer therapy: what does the experimental and clinical data tell us? *Cancer Biol. Ther*. **2** 477–490

Brown JM and Wouters BG 1999 Apoptosis, p53, and tumor cell sensitivity to anticancer agents. *Cancer Res*. **59** 1391–1399

Brown DM, Kelly GE and Husband AJ 2005 Flavonoid compounds in maintenance of prostate health and prevention and treatment of cancer. *Mol. Biotechnol*. **30** 253–270

Cheng EH, Wei MC, Weiler S, Flavell RA, Mak TW, Lindsten T and Korsmeyer SJ 2001 BCL-2, BCL-X(L) sequester BH3 domain-only molecules preventing BAX- and BAK-mediated mitochondrial apoptosis. *Mol. Cell* **8** 705–711

Constantinou AI, Mehta R and Husband A 2003 Phenoxodiol, a novel isoflavone derivative, inhibits dimethylbenz[a]anthracene (DMBA)-induced mammary carcinogenesis in female Sprague-Dawley rats. *Eur. J. Cancer* **39** 1012–1018

Cory S and Adams JM 2002 The Bcl2 family: regulators of the cellular life-or-death switch. *Nat. Rev. Cancer* **2** 647–656

De Luca T, Morre DM, Zhao H and Morre DJ 2005 NAD+/NADH and/or CoQ/CoQH2 ratios from plasma membrane electron transport may determine ceramide and sphingosine-1-phosphate levels accompanying G1 arrest and apoptosis. *Biofactors* **25** 43–60

Dharmarajan AM, Goodman SB, Tilly KI and Tilly JL 1994 Apoptosis during functional corpus luteum regression: evidence of a role for chorionic gonadotropin in promoting luteal cell survival. *Endocrine J.* **2** 295–303

Feldman BJ and Feldman D 2001 The development of androgen-independent prostate cancer. *Nat. Rev. Cancer* **1** 34–45

Fojo T and Bates S 2003 Strategies for reversing drug resistance. *Oncogene* **22** 7512–7523

Gamble JR, Xia P, Hahn CN, Drew JJ, Drogemuller CJ, Brown D and Vadas MA 2005 Phenoxodiol, an experimental anticancer drug, shows potent antiangiogenic properties in addition to its antitumour effects. *Int. J. Cancer* **118** 2412–2420

Georgaki S, Skopeliti M, Tsiatas M, Nicolaou KA, Ioannou K, Husband A, Bamias A, Dimopoulos MA, *et al.* 2009 Phenoxodiol, an anticancer isoflavene, induces immunomodulatory effects *in vitro* and *in vivo*. *J. Cell Mol. Med*. **13** 3929–3938

Gleave M, Miyake H and Chi K 2005 Beyond simple castration: targeting the molecular basis of treatment resistance in advanced prostate cancer. *Cancer Chemother. Pharmacol*. **56** 47–57

Hong SJ, Dawson TM and Dawson VL 2004 Nuclear and mitochondrial conversations in cell death: PARP-1 and AIF signaling. *Trends Pharmacol. Sci*. **25** 259–264

Hsing AW, Tsao L and Devesa SS 2000 International trends and patterns of prostate cancer incidence and mortality. *Int. J. Cancer* **85** 60–67

Jemal A, Murray T, Ward E, Samuels A, Tiwari RC, Ghafoor A, Feuer EJ and Thun MJ 2005 Cancer statistics 2005 *CA Cancer J. Clin*. **55** 10–30

Kamsteeg M, Rutherford T, Sapi E, Hanczaruk B, Shahabi S, Flick M, Brown D and Mor G 2003 Phenoxodiol—an isoflavone analog—induces apoptosis in chemoresistant ovarian cancer cells. *Oncogene* **22** 2611–2620

Korsmeyer SJ, Wei MC, Saito M, Weiler S, Oh KJ and Schlesinger PH 2000 Pro-apoptotic cascade activates BID, which oligomerizes BAK or BAX into pores that result in the release of cytochrome c. *Cell Death Differ*. **7** 1166–1173

McPherson RA, Galettis PT and de Souza PL 2009 Enhancement of the activity of phenoxodiol by cisplatin in prostate cancer cells. *Br. J. Cancer* **100** 649–655

Middleton E Jr, Kandaswami C and Theoharides TC 2000 The effects of plant flavonoids on mammalian cells: implications for inflammation, heart disease, and cancer. *Pharmacol Rev*. **52** 673–751

Morre DJ, Chueh PJ, Yagiz K, Balicki A, Kim C and Morre DM 2007 ECTO-NOX target for the anticancer isoflavene phenoxodiol. *Oncol. Res*. **16** 299–312

Puthalakath H and Strasser A 2002 Keeping killers on a tight leash: transcriptional and post-translational control of the pro-apoptotic activity of BH3-only proteins. *Cell Death Differ*. **9** 505–512

Ruth AC and Roninson IB 2000 Effects of the multidrug transporter P-glycoprotein on cellular responses to ionizing radiation. *Cancer Res*. **60** 2576–2578

Sapi E, Alvero AB, Chen W, O'Malley D, Hao XY, Dwipoyono B, Garg M, Kamsteeg M, *et al.* 2004. Resistance of ovarian carcinoma cells to docetaxel is XIAP dependent and reversible by phenoxodiol. *Oncol. Res*. **14** 567–578

Scherr DS, Vaughan ED Jr, Wei J, Chung M, Felsen D, Allbright R and Knudsen BS 1999 BCL-2 and p53 expression in clinically localized prostate cancer predicts response to external beam radiotherapy. *J. Urol*. **162** 12–16; discussion 16–17

Silasi DA, Alvero AB, Rutherford TJ, Brown D and Mor G 2009 Phenoxodiol: pharmacology and clinical experience in cancer monotherapy and in combination with chemotherapeutic drugs. *Expert Opin. Pharmacother*. **10** 1059–1067

Tang Y, Khan MA, Goloubeva O, Lee DI, Jelovac D, Brodie AM and Hussain A 2006 Docetaxel followed by castration improves outcomes in LNCaP prostate cancer-bearing severe combined immunodeficient mice. *Clin. Cancer Res*. **12** 169–174

Tannock IF and Lee C 2001 Evidence against apoptosis as a major mechanism for reproductive cell death following treatment of cell lines with anti-cancer drugs. *Br. J. Cancer* **84** 100–105

Tannock IF, de Wit R, Berry WR, Horti J, Pluzanska A, Chi KN, Oudard S, Theodore C, *et al.* 2004 Docetaxel plus prednisone or mitoxantrone plus prednisone for advanced prostate cancer. *New Engl. J. Med*. **351** 1502–1512

MS received 26 July 2011; accepted 20 October 2011

Corresponding editor: RITA MULHERKAR